Available online at www.sciencedirect.com

ScienceDirect

Current Opinion in Electrochemistry

Review Article

Pitfalls in X-ray absorption spectroscopy analysis and interpretation: A practical guide for general users

Maoyu Wang and Zhenxing Feng

Abstract

Despite the growing popularity of X-ray absorption spectroscopy (XAS) in scientific research, many researchers do not receive formalized training on this technique. Some of them learned from online resources, which only briefly introduce XAS and its applications. Here, this article aims to provide the overview of tips about the XAS analysis, general rules, as well as required information for presenting XAS data in publications, and some common mistakes in XAS data interpretations. Armed with these basics, the motivated aspiring XAS researchers will find existing resources more accessible and can progress much faster in understanding and using XAS.

Addresses

School of Chemical, Biological, and Environmental Engineering, Oregon State University, Corvallis, OR, 97331, USA

Corresponding author: Feng, Zhenxing (zhenxing.feng@oregonstate.edu)

Current Opinion in Electrochemistry 2021, **30**:100803

This review comes from a themed issue on **Electrocatalysis (2021)**

Edited by **Zichuan J. Xu**

For a complete overview see the Issue and the Editorial

Available online 8 July 2021

https://doi.org/10.1016/j.coelec.2021.100803

2451-9103/© 2021 Elsevier B.V. All rights reserved.

Keywords

X-ray absorption spectroscopy, Oxidation state, Local structure, *In-situ*, *Operando*, Misinterpretation.

Introduction

The electronic structure and local geometric arrangements are important information in materials science research. Among many characterization methods, X-ray absorption spectroscopy (XAS) is a unique technique that can provide element-specific information such as electronic structure, oxidization states, and local coordination environment without strict requirements on sample preparation [1,2]. The fast development of synchrotron X-ray sources (about 92 synchrotron sources around the world) has allowed the wide applications of XAS [3]. Recently, XAS can also be performed on the benchtop instrument, making it more accessible in the laboratory [4,5].

Comparing with other characterization techniques such as scanning transmission electron microscopy and X-ray photoelectron spectroscopy, which are limited in the vacuum condition, the continuously tunable hard XAS (energy higher than 5 keV) can be operated at ambient condition (i.e. 1 atm), which is beneficial for XAS measurements in various environments. The designed electrochemical cells allow the operation of XAS experiments in reaction conditions, *[6,7] thus enabling *in situ*/*operando* monitoring of the materials' change (e.g. electrocatalyst restructuring) under the real conditions [8,9]. XAS can be operated in three different detection modes (transmission, fluorescence, and electron yield) for various systems, not only homogenously concentrated materials such as metal alloy, metal oxides, and nanoparticles but also inhomogeneous, dilute, or atomically dispersed materials [10–12]. The electron yield mode and gracing-incident XAS could even be used to probe the surface information of monolayer thin films [13,14].

Owing to those advantages of XAS, some researchers blindly use it to study materials' chemical states and local structures without proper data analysis and sometimes misinterpret XAS results. For the oxidization state comparison, it is necessary to have well-chosen references to compare, and for the local structure analysis the fitting model needs to be built on well-defined crystal structures. The more one has known about materials in measurements, the more helpful XAS will be. Many literatures have reviewed the XAS fundaments and its applications in electrocatalyst [15–17], including our recent review on *in situ* XAS study of the nanoscale electrocatalyst to obtain nanocluster size information, element site occupation, oxidization state, and so on [3]. To help the science community properly use XAS in research, this article will go over the standard procedures for analyzing and presenting XAS data, and discuss some common mistakes in XAS analysis. Examples are mainly from hard XAS studies. We assume that readers already have some knowledge preparation in XAS or similar techniques (e.g. electron energy loss spectroscopy). In addition, we will briefly talk about the difference between *in situ* and *operando* because the two conditions are not well differentiated in many publications.

X-ray absorption near-edge structure

X-ray absorption near-edge structure (XANES) refers to the edge jump region in XAS spectrum, which is commonly used to evaluate the oxidization state of the detected materials [11,12]. Because XAS is an element-specific technique based on the Beer's law [11,12], different elements have different absorption energies. Due to the tunable synchrotron X-ray energy range, the K-edge and L-edge (including L2 and L3) are the two most commonly measured absorption edges [18–20]. K-edge is often used for the 3d and 4d transition metals such as Fe, Co, Mo, Pd, and Ru [21–25], and L-edge is often used for the 5d and 6p metals such as Ir, Pt, Au, and Bi [9,26–28]. The different absorption edges need different methods to estimate the oxidization states. For example, the position of the half height of the edge rise (the so-called edge position) is commonly used in evaluating K-edge oxidation state [29–33]. Figure 1a shows that the edge position of higher oxidation state of Co shifts toward higher energy [22]. Sometimes the edge position method may not work, and the first derivations of XANES spectra and the peak positions can be used to compare the oxidation state of the elements, as shown in Figure 1b,c for determining the Cu oxidization states [34]. Besides the above three strategies, Dau et al. [32] suggested an integration method to estimate the XANES oxidization state. By integrating the XANES area under the edge from $\mu = 0.1$ to 1, the center of the mass of this integrated area is good for comparing the oxidation states of the measured elements. They also pointed out that the integration approach is more accurate than edge position and the derivation methods [32].

Unlike the K-edge XANES, the absorption peak position and peak intensity in L-edge XANES are mostly used to quantify the elements' oxidization states instead of the absorption edge position. For example, Minguzzi et al.

Figure 1

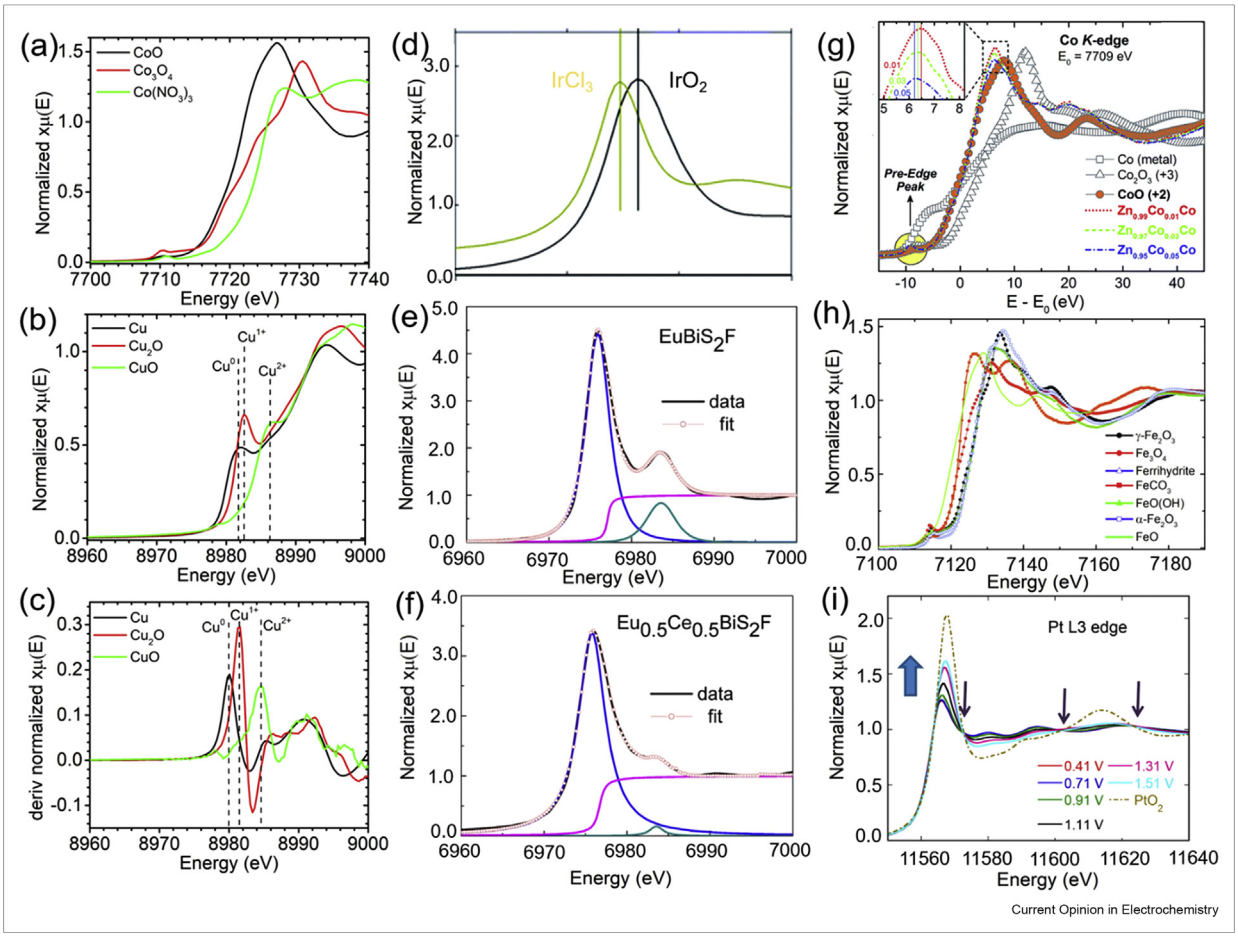

(**a**) Co K-edge XANES of several references [24]. (**b**) Cu K-edge XANES of Cu references [34]. (**c**) The first derivation of Cu K-edge XANES [34]. (**d**) Ir L3-edge XANES of Ir(III) and Ir(IV) references [35]. (**e**) Eu L3-edge XANES of $EuBiS_2F$ [39] and (**f**) Eu L3-edge XANES of $Eu_{0.5}Ce_{0.5}BiS_2F$ [39], where the raw data, simulated peaks, and the sum of the simulations are denoted by circle, solid lines, and solid black line. (**g**) Co K-edge XANES with peak intensity analysis [47]. (**h**) Fe K-edge XANES of series of Fe references with different Fe oxidization state [45]. (**i**) Pt L3-edge XANES of Pt nanoparticle at different applied potentials [28].

[35] chose the peak position to estimate Ir oxidization state (Figure 1d). In some cases, XANES spectrum has complicated shapes and multiple peaks, and the peak fitting method could be better for estimating the oxidation state. XANES spectrum can be generally decomposed to one or several Gaussian peaks plus an arctan shape [36—38]. The arctan function is to mimic the edge jump and the peak positions and/or the peak areas of these Gaussian peaks are to quantify the different oxidation states and the ratios [36—38]. This method has been reported to estimate Eu oxidization state (Figure. 1e,f) accurately, where the peak around 6975 eV stands for Eu(II) and the peak around 6983 eV stands for Eu(III) [39].

Because the XANES is related to the excitation of core electron(s) to unoccupied states, the electronic configuration can influence the shape of XANES, thus providing information of the element's electronic and chemical structure [33,40]. Soft XAS (energy lower than 2 keV) is powerful to characterize detailed electronic structure such as the orbital spin and splitting for 3d transition metal, the transition metal—oxygen covalency, and 3d transition metal oxidization state [22,24,41]. Due to the complicity in electronic structure, only some simple comparison/analysis can be done on soft XAS data and theoretical simulation is necessary to extract deep insights. This is same for hard XAS, which is less sensitive than soft XAS in electronic structure study partly due to weaker energy resolution. However, in some cases, qualitative structure information can also be obtained in hard XAS. For example, the forbidden 1s→3d transition would present in the 3d transition metal K-edge XANES pre-peaks due to the symmetry breaking in local structure [30]. The lower symmetry leads to higher pre-peak intensity, which is best demonstrated in XANES of V_2O_5 (distorted VO_5 pyramid structure) and VO_2 (distorted VO_6 octahedral structure) [42]. Moreover, the different atoms have different attraction ability for electrons. This electronegativity can influence the electronic structure around the detected atoms, which could also affect the edge position or peak shape in XANES (Figure 1h) [30,43,44]. Kuzmin and Chaboy [45] show that the Fe with the same oxidization state can have different edge shifts and edge shapes (Figure 1h). That is why we need a well-established standard system to obtain correct information of the oxidization states. Furthermore, the white line intensity is also another common feature mentioned in the XAS paper. Some researchers may use the white line intensity in K-edge XANES to discuss the number of electrons or empty states in the 3d orbitals of the transition metals for arguing about the oxidization state. However, the K-edge is an s→p transition, which would not give any information about 3d orbitals (valence state in 3d transition metals) [11,12,44]. Only when the transition metal 3d orbitals is hybridized with the p orbitals of other bonding atoms such as O and S, the peak intensity can tell some information indirectly about the electron occupation in the antibonding and bonding states (Figure 1g) [46,47]. The decreases in peak intensity and shift to lower energies (Figure 1g, inset) suggest an increase in the empty states [47]. However, the story would be different in L-edge XANES because it is the p→d transitions [11,12]. The L-edge XANES can thus be used to characterize the electron occupation in d orbitals (Figure 1I). The increased white line intensity around 11,570 eV indicates more oxides formation and less electron filling of d-band (Figure 1I) [27]. Furthermore, one should be cautious to use the peak intensity because the self-absorption could also influence it, especially when materials are too thick for the fluorescence measurement [11,12,44]. The self-absorption may be corrected if the composition of the sample is known [48]. Overall, XANES could tell more information than the oxidization state but it needs to be treated carefully case by case.

Extended X-ray absorption fine structure

Extended X-ray absorption fine structure (EXAFS) provides the information about the local structure including coordination numbers and bonding lengths [11,12,44]. Some researchers only present the R-space EXAFS spectra [27,49], which are smooth curves with zero noise-to-signal ratio to reflect the real-space bonding intuitively (Figure 2a). However, they are the Fourier transformation of the part of the measured data in k-space with different k-weights (Figure 2b). The blind comparison of R-space EXAFS is inaccurate, misleading, and sometimes meaningless. The range of EXAFS in k-space also determines the real-space spatial resolution and the analyzable range of the local ordering. In an XAS experiment, it is recommended to measure as far as 12 $Å^{-1}$ or at least 10 $Å^{-1}$ for the first-shell analysis (e.g. up to 2—2.5 Å local ordering in real space). Higher shell (e.g. second shell around 3 Å) analysis requires k-space measurements more than 12.5 $Å^{-1}$. For EXAFS modeling, the good fitting in R-space does not necessarily mean a reasonable fit in k-space (Figure 2c,d). This is because the Fourier transformation with different k-weights can diminish some misfits in k-space. Therefore, both original k-space and R-space spectra should be presented in the publication to show the data quality and the goodness of fitting.

Two other important pieces of information commonly missing in the publications are the EXAFS fitting procedures and fitting parameters. When one runs the EXAFS fitting, it is necessary to have a standard or well-defined material from similar structure systems to help estimate the coordination number. The inappropriate standards would give wrong structure information [11,12]. Furthermore, all fitting parameters such as the

coordination number (N), scattering length (R or ΔR), mean square disorder (σ^2), the difference to the initial absorption edge energy (ΔE_0), and amplitude reduction factor (S_0^2) have physical meaning and errors [11,12]. The reporting of the fitting procedures and all parameters with errors can help readers judge how good and reasonable the EXAFS analysis is [11,12]. In addition, if the materials are studied under different conditions or a set of similar materials are studied together, it is better to make the same EXAFS fitting procedures (fitting range, Fourier transformation range, and k-weight) for those materials [11,12].

Besides missing information in the publications, there are some misinterpretations of EXAFS results. Many researchers use the peak intensity in the R-space EXAFS to talk about the coordination numbers, which is inaccurate. Based on the EXAFS theory, the peak intensity is convoluted with the coordination number and the mean square disorder, and could also be affected by the self-absorption [11,12]. For example, both FeO and Fe_2O_3 have six oxygen coordinated in the first shell, but the FeO has much low Fe—O peak intensity (~1.5 Å) than that of Fe_2O_3 (Figure 2e). If the measurements are done on one material at different conditions, the direct comparison of EXAFS spectra may be suitable [9,34,50,51]. Otherwise, such discussions need to be done with caution. It is strongly suggested to use EXAFS fitting results to compare and discuss the coordination numbers [11,12]. Moreover, it is noted that the scattering length (*R*) obtained from the EXAFS analysis is the X-ray passing distances between atoms and may not be the bonding lengths [11,12]. Only when the scattering is a single scattering between two atoms, the scattering length is equal to the bonding length.

Nowadays, singly dispersed catalyst is a scorching topic in electrochemical research. Many researchers tried to use EXAFS to confirm metal—Z_x (Z = C, N, and O, and x is an integral number) motifs [29,52]. However, it is challenging for EXAFS to distinguish the scattering between elements with a close atomic number, such as Fe—C and Fe—N scattering. Even with the two-dimensional wavelet transform, it is still difficult to differentiate those scattering paths. For example, the wavelet transform of Co EXAFS is still hard to tell whether it is Co—O bond or Co—N bond (Figure 2f) [1]. Another problem is the determination of the exact coordination environment such as FeN_5 [53,54]. Note that there are errors associated with coordination number from EXAFS analysis. In particular, some singly dispersed materials have low concentration (less than 1 at%), resulting in poor data quality and then large errors in EXAFS fitting [11,12,44]. Thus, the discussion

Figure 2

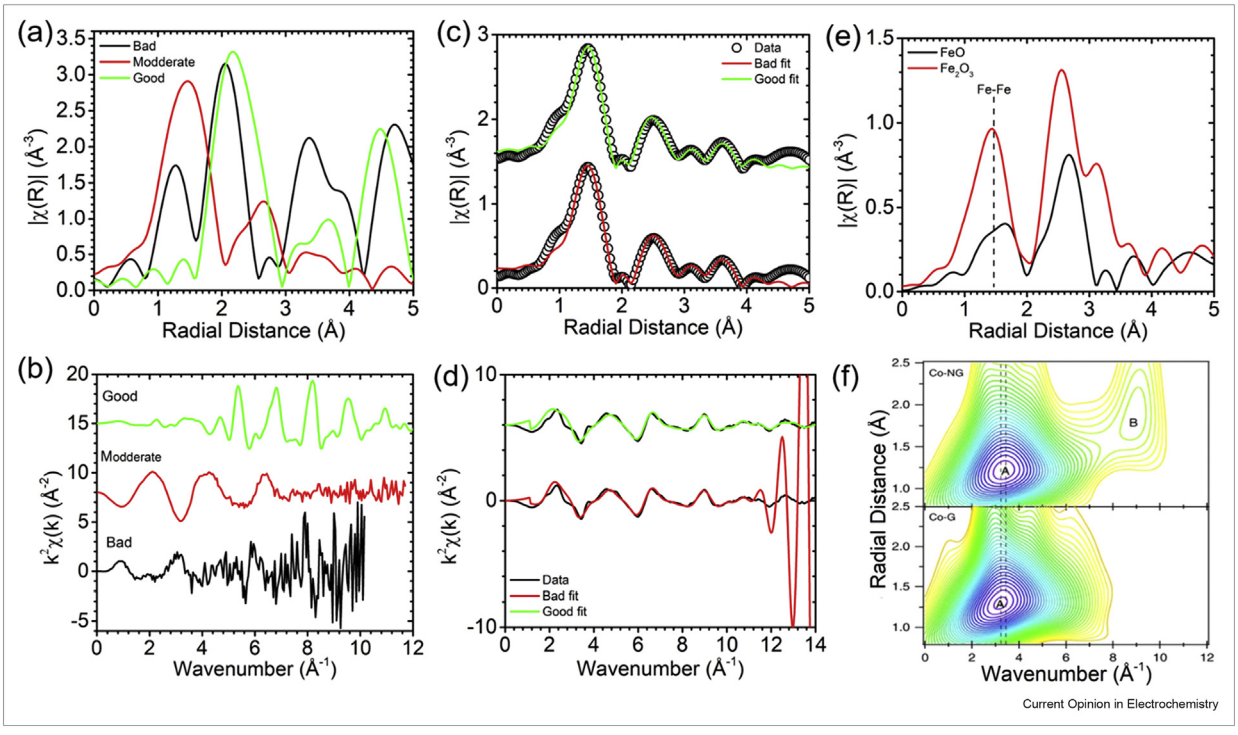

(**a**) Some examples of Fourier-transformed R-space EXAFS spectra and (**b**) k-space EXAFS data. (**c**) Fourier-transformed R-space EXAFS data and fitting, where the black circles are data and the solid lines are fitted results, and (**d**) k-space EXAFS data and fitting, where the black lines are data, and the red/green lines are fitted results. (**e**) Fe K-edge Fourier-transformed R-space EXAFS of two 6 coordinated Fe references. (**f**) Wavelet transform of the Co K-edge k^3-weighted EXAFS results, where the dash line stands for Co–O/N bonding [1].

related to the exact coordination number should be conservative, and it is suggested to use multimodal characterizations for confirming the local structure.

In situ versus *operando*

The use of XAS in reaction conditions for structural and chemical analysis becomes more and more popular. However, the terms *in situ* and *operando* are not well explained in publications. Miguel Bañares has pointed out that the *operando* methodology combines structure and activity measurements in a single experiment, using a reaction cell that meets the requirements for both, a catalytic reactor and an *in situ* cell [55]. This means that *operando* experiments have the strictest requirements and mainly focus on the study of the transient states, or measurements under a non-stop reaction. In contrast, the *in situ* methodology only emphasizes the measurement of materials' structure under reaction conditions and does not measure activity or perform property tests in the same experiment. As long as the main features of the property tests can be reproduced in *in situ* experiments, the characterizations can reflect the reaction-induced changes in materials. This broadly defines that *in situ* measurements can be done even when the reaction is paused. For example, Weng et al. [34] used an *in situ* cell for studying CuPc electrocatalyst during the electrochemical carbon dioxide reduction. They carried out *in situ* XAS measurements at certain potentials when the steady state current has been achieved, which is thermodynamically stable and controlled by the reaction kinetics [34]. Sometimes *in situ* measurements are even carried out when the materials are moved out of the reactor, by ensuring that the same reaction can be resumed after the materials are moved back. *Operando* is part of *in situ* but the opposite is not true. Typical XAS may not meet the *operando* requirements due to long data collection time. However, the time-resolved XAS or recently developed quick XAS is useful to probe the dynamic change with the time resolution to couple seconds or even femtoseconds (e.g. pump-probe) in an *operando* experiment [56–58]. Lin et al. [57] reported an *operando* time-resolved XAS to reveal the chemical nature which enables highly selective carbon dioxide reduction. Compared to the traditional XAS measurements, the time-resolved XAS can collect the spectrum with a sub-second time resolution which can quickly probe the electrochemical steady condition at a time-scale of seconds or few minutes [57]. However, this experiment is still not the true *operando* because the XAS was measured at certain selected reaction points instead of the regular cyclic voltammetry. A lot of *operando* measurements (e.g. XANES) on batteries were performed during continuous galvanometric charging and discharging processes, which are the same as the cells tested in normal electrochemical condition. For example, the experiment carried out by Liu et al. [59] demonstrated the real *operando* soft XAS. They measured the lithium-ion and electron dynamics in $Li(Co_{1/3}Ni_{1/3}Mn_{1/3})O_2$ and $LiFePO_4$ cathodes in polymer electrolytes during the charging and discharging cycling.

Conclusion

XAS is a unique characterization technique to understand the material's oxidation state and local structure information. However, it is necessary to have well-defined standards to gain useful information from XAS, and sometimes the theoretical modeling is very helpful to analyze the XAS spectra for extracting useful electronic and atomic structure information. It may not be good enough to perform XAS alone, and multimodal characterizations are strongly recommended. Comprehensive information would make the interpretation of XAS results more convincing and trustable. Besides the practical guides provided in this short review, we also suggest general users to rely on some open forums such as Demeter GitHub and xafs.org for help on some specific problems. With the continuous development of advanced synchrotron facilities, benchtop XAS spectrometer, and the XAS technique itself, we believe that XAS will become more and more powerful and popular in scientific research.

Declaration of competing interest

The authors declare that they have no known competing financial interests or personal relationships that could have appeared to influence the work reported in this paper.

Acknowledgement

This work was supported by the National Science Foundation under Grant Nos. CBET-1949870, CBET-2016192, and DMR-1832803.

References

Papers of particular interest, published within the period of review, have been highlighted as:

* of special interest

1. * Fei HL, Dong JC, Arellano-Jimenez MJ, *et al.*: **Atomic cobalt on nitrogen-doped graphene for hydrogen generation**. *Nat Commun* 2015, **6**:8668.
2. Wei C, Feng ZX, Scherer GG, *et al.*: **Cations in octahedral sites: a descriptor for oxygen electrocatalysis on transition-metal spinels**. *Adv Mater* 2017, **29**:1606800.
3. Wang MY, Arnadottir L, Xu ZCJ, Feng ZX: **In situ X-ray absorption spectroscopy studies of nanoscale electrocatalysts**. *Nano-Micro Lett* 2019, **11**:47.
4. Jahrman EP, Holden WM, Ditter AS, *et al.*: **An improved laboratory-based x-ray absorption fine structure and x-ray emission spectrometer for analytical applications in materials chemistry research**. *Rev Sci Instrum* 2019, **90**, 024106.
5. Zimmermann P, Peredkov S, Abdala PM, *et al.*: **Modern X-ray spectroscopy: XAS and XES in the laboratory**. *Coord Chem Rev* 2020, **423**:213466.
6. Wang HY, Hung SF, Hsu YY, *et al.*: **In situ spectroscopic identification of mu-OO bridging on spinel Co3O4 water oxidation electrocatalyst**. *J Phys Chem Lett* 2016, **7**:4847–4853.

7. Wang DN, Zhou JG, Hu YF, *et al.*: **In situ X-ray absorption near-edge structure study of advanced NiFe(OH)$_x$ electrocatalyst on carbon paper for water oxidation**. *J Phys Chem C* 2015, **119**:19573–19583.
8. Zhang X, Wang Y, Gu M, *et al.*: **Molecular engineering of dispersed nickel phthalocyanines on carbon nanotubes for selective CO_2 reduction**. *Nat Energy* 2020, **5**:684–692.
9. Cai C, Wang MY, Han SB, *et al.*: **Ultrahigh oxygen evolution reaction activity achieved using Ir single atoms on amorphous CoO_x nanosheets**. *ACS Catal* 2021, **11**:123–130.
10. Nelson RC, Miller JT: **An introduction to X-ray absorption spectroscopy and its in situ application to organometallic compounds and homogeneous catalysts**. *Catal Sci Technol* 2012, **2**:461–470.
11. Calvin S: *XAFS for everyone*. Hoboken: CRC Press; 2013.
12. Bunker G: *Introduction to XAFS : a practical guide to x-ray absorption fine structure spectroscopy*. Cambridge: Cambridge University Press; 2010.
13. Gunduz S, Deka DJ, Kim J, *et al.*: **Incident-angle dependent operando XAS cell design: investigation of the electrochemical cells under operating conditions at various incidence angles**. *RSC Adv* 2021, **11**:6456–6463.
14. Maurizio C, Rovezzi M, Bardelli F, *et al.*: **Setup for optimized grazing incidence x-ray absorption experiments on thin films on substrates**. *Rev Sci Instrum* 2009, **80**, 063904.
15. Lassalle-Kaiser B, Gul S, Kern J, *et al.*: **In situ/Operando studies of electrocatalysts using hard X-ray spectroscopy**. *J Electron Spectrosc* 2017, **221**:18–27.
16. Fabbri E, Abbott DF, Nachtegaal M, Schmidt TJ: **Operando X-ray absorption spectroscopy: a powerful tool toward water splitting catalyst development**. *Curr Opin Electroche* 2017, **5**:20–26.
17. Timoshenko J, Cuenya BR: **In situ/operando electrocatalyst characterization by X-ray absorption spectroscopy**. *Chem Rev* 2021, **121**:882–961.
18. Lu QY, Chen Y, Bluhm H, Yildiz B: **Electronic structure evolution of $SrCoO_x$ during electrochemically driven phase transition probed by in situ X-ray spectroscopy**. *J Phys Chem C* 2016, **120**:24148–24157.
19. Kaito T, Mitsumoto H, Sugawara S, *et al.*: **K-edge X-ray absorption fine structure analysis of Pt/Au core-shell electrocatalyst: evidence for short Pt-Pt distance**. *J Phys Chem C* 2014, **118**:8481–8490.
20. Vagnini MT, Mara MW, Harpham MR, *et al.*: **Interrogating the photogenerated Ir(IV) state of a water oxidation catalyst using ultrafast optical and X-ray absorption spectroscopy**. *Chem Sci* 2013, **4**:3863–3873.
21. Pattengale B, Huang YC, Yan XX, *et al.*: **Dynamic evolution and reversibility of single-atom Ni(II) active site in 1T-MoS2 electrocatalysts for hydrogen evolution**. *Nat Commun* 2020, **11**:4114.
22. Wang XX, Cullen DA, Pan YT, *et al.*: **Nitrogen-coordinated single cobalt atom catalysts for oxygen reduction in proton exchange membrane fuel cells**. *Adv Mater* 2018, **30**:1706758.
23. Hu C, Song EH, Wang MY, *et al.*: **Partial-single-Atom, partial-nanoparticle composites enhance water dissociation for hydrogen evolution**. *Adv Sci* 2021, **8**:2001881.
24. Zhang HG, Hwang S, Wang MY, *et al.*: **Single atomic iron catalysts for oxygen reduction in acidic media: particle size control and thermal activation**. *J Am Chem Soc* 2017, **139**:14143–14149.
25. Huynh TT, Tsai MC, Pan CJ, *et al.*: **Synergetic electrocatalytic activities towards hydrogen peroxide: understanding the ordered structure of PdNi bimetallic nanocatalysts**. *Electrochem Commun* 2019, **101**:93–98.
26. Gong QF, Ding P, Xu MQ, *et al.*: **Structural defects on converted bismuth oxide nanotubes enable highly active electrocatalysis of carbon dioxide reduction**. *Nat Commun* 2019, **10**:2807.
27. Sasaki K, Marinkovic N, Isaacs HS, Adzic RR: **Synchrotron-based in situ characterization of carbon-supported platinum and platinum monolayer electrocatalysts**. *ACS Catal* 2016, **6**:69–76.
28. Rodriguez JA, Hanson JC, Stacchiola D, Senanayake SD: **In situ/operando studies for the production of hydrogen through the water-gas shift on metal oxide catalysts**. *Phys Chem Chem Phys* 2013, **15**:12004–12025.
29. Yang HB, Hung SF, Liu S, *et al.*: **Atomically dispersed Ni(I) as the active site for electrochemical CO_2 reduction**. *Nat Energy* 2018, **3**:140–147.
30. Gholam T, Zheng LR, Wang JO, *et al.*: **Synchrotron X-ray absorption spectroscopy study of local structure in Al-doped BiFeO3 powders**. *Nanoscale Res Lett* 2019, **14**:137.
31. Sawama Y, Ban K, Akutsu-Suyama K, *et al.*: **Birch-type reduction of arenes in 2-propanol catalyzed by zero-valent iron and platinum on carbon**. *ACS Omega* 2019, **4**:11522–11531.
32. Dau H, Liebisch P, Haumann M: **X-ray absorption spectroscopy to analyze nuclear geometry and electronic structure of biological metal centers - potential and questions examined with special focus on the tetra-nuclear manganese complex of oxygenic photosynthesis**. *Anal Bioanal Chem* 2003, **376**:562–583.
33. Chen WT, Hsu CW, Lee JF, *et al.*: **Theoretical analysis of Fe K-edge XANES on iron pentacarbonyl**. *ACS Omega* 2020, **5**:4991–5000.
34. Weng Z, Wu Y, Wang M, *et al.*: **Active sites of copper-complex catalytic materials for electrochemical carbon dioxide reduction**. *Nat Commun* 2018, **9**:415.
35. Minguzzi A, Lugaresi O, Achilli E, *et al.*: **Observing the oxidation state turnover in heterogeneous iridium-based water oxidation catalysts**. *Chem Sci* 2014, **5**:3591–3597.
36. Shimizu K, Kamiya Y, Osaki K, *et al.*: **The average Pd oxidation state in Pd/SiO_2 quantified by L_3-edge XANES analysis and its effects on catalytic activity for CO oxidation**. *Catal Sci Technol* 2012, **2**:767–772.
37. Fujishiro H, Naito T, Takeda D, *et al.*: **Simultaneous valence shift of Pr and Tb ions at the spin-state transition in $(Pr_{1-y}Tb_y)_{0.7}Ca_{0.3}CoO_3$**. *Phys Rev B* 2013, **87**:155153.
38. Sundermann M, Strigari F, Willers T, *et al.*: **$CeRu_4Sn_6$: a strongly correlated material with nontrivial topology**. *Sci Rep-Uk* 2015, **5**:17937.
39. Cheng J, Zhai HF, Wang Y, *et al.*: **Role of valence changes and nanoscale atomic displacements in BiS_2-based superconductors**. *Sci Rep-Uk* 2016, **6**:37394.
40. Chalmin E, Farges F, Brown G: **A pre-edge analysis of Mn K-edge XANES spectra to help determine the speciation of manganese in minerals and glasses**. *Contrib Mineral Petrol* 2009, **157**:111–126.
41. Suntivich J, Hong WT, Lee YL, *et al.*: **Estimating hybridization of transition metal and oxygen states in perovskites, from O K-edge X-ray absorption spectroscopy**. *J Phys Chem C* 2014, **118**:1856–1863.
42. Feng Z, Ma Q, Lu J, *et al.*: **Atomic-scale cation dynamics in a monolayer VO_X/α-Fe_2O_3 catalyst**. *RSC Adv* 2015, **5**:103834–103840.
43. Zandkarimi B, Sun G, Halder A, *et al.*: **Interpreting the operando XANES of surface-supported subnanometer clusters: when fluxionality, oxidation state, and size effect fight**. *J Phys Chem C* 2020, **124**:10057–10066.
44. Newville M: **Fundamentals of XAFS**. *Rev Mineral Geochem* 2014, **78**:33–74.
45. Kuzmin A, Chaboy J: *EXAFS and XANES analysis of oxides at the nanoscale*, **1**. IUCrJ; 2014:571–589.
46. de Souza TE, Mesquita A, de Zevallos AO, *et al.*: **Structural and magnetic properties of dilute magnetic oxide based on nanostructured Co-doped anatase TiO_2 ($Ti_{1-x}Co_xO_{2-\delta}$)**. *J Phys Chem C* 2013, **117**:13252–13260.
47. Valerio LR, Mamani NC, de Zevallos AO, *et al.*: **Preparation and structural-optical characterization of dip-coated**

nanostructured Co-doped ZnO dilute magnetic oxide thin films. *RSC Adv* 2017, **7**:20611–20619.

48. Ravel B, Athena M Newville, Artemis Hephaestus: **Data analysis for X-ray absorption spectroscopy using IFEFFIT**. *J Synchrotron Radiat* 2005, **12**:537–541.

49. Witkowska A, Dsoke S, Principi E, *et al.*: **Pt-Co cathode electrocatalyst behaviour viewed by in situ XAFS fuel cell measurements**. *J Power Sources* 2008, **178**:603–609.

50. Birhanu MK, Tsai MC, Kahsay AW, *et al.*: **Copper and copper-based bimetallic catalysts for carbon dioxide electroreduction**. *Adv Mater Interf* 2018, **5**:1800919.

51. Friebel D, Miller DJ, O'Grady CP, *et al.*: **In situ X-ray probing reveals fingerprints of surface platinum oxide**. *Phys Chem Chem Phys* 2011, **13**:262–266.

52. Li JZ, Chen MJ, Cullen DA, *et al.*: **Atomically dispersed manganese catalysts for oxygen reduction in proton-exchange membrane fuel cells**. *Nat Catal* 2018, **1**:935–945.

53. Zhao Y-M, Zhang P-C, Xu C, *et al.*: **Design and preparation of Fe–N_5 catalytic sites in single-atom catalysts for enhancing the oxygen reduction reaction in fuel cells**. *ACS Appl Mater Interfaces* 2020, **12**:17334–17342.

54. Cheng H, Wu X, Li X, *et al.*: **Zeolitic imidazole framework-derived FeN_5-doped carbon as superior CO2 electrocatalysts**. *J Catal* 2021, **395**:63–69.

55. Banares MA: **Operando spectroscopy - preface**. *Catal Today* 2007, **126**:1–2.

56. Cheaib K, Maurice B, Mateo T, *et al.*: **Time-resolved X-ray absorption spectroelectrochemistry of redox active species in solution**. *J Synchrotron Radiat* 2019, **26**:1980–1985.

57. Lin SC, Chang CC, Chiu SY, *et al.*: **Operando time-resolved X-ray absorption spectroscopy reveals the chemical nature enabling highly selective CO_2 reduction**. *Nat Commun* 2020, **11**:3525.

58. Bak SM, Shadike Z, Lin RQ, *et al.*: **In situ/operando synchrotron-based X-ray techniques for lithium-ion battery research**. *NPG Asia Mater* 2018, **10**:563–580.

59. Liu X, Wang D, Liu G, *et al.*: **Distinct charge dynamics in battery electrodes revealed by in situ and operando soft X-ray spectroscopy**. *Nat Commun* 2013, **4**:2568.